

1 **Deposit-feeding of *Nonionellina labradorica* (-foraminifera) from an**
2 **Arctic methane seep site and possible association with a**
3 **methanotroph ~~revealed by transmission electron microscopy~~**

4 Christiane Schmidt^{1,2,3}, Emmanuelle Geslin¹, Joan M Bernhard⁴, Charlotte LeKieffre^{1,5}, Mette
5 Marianne Svenning^{2,6}, Helene Roberge^{1,7}, Magali Schweizer¹, Giuliana Panieri²

6 ¹LPG, Laboratoire de Planétologie et de Géodynamique Géosciences, Univ. of Angers, Nantes Université de Nantes,
7 Le Mans Univ CNRS, LPG, SFR QUASAV, Angers, 49000, France

8 ²CAGE, Centre for Arctic Gas Hydrate, Environment and Climate, UiT, The Arctic University of Norway, Tromsø,
9 9010, Norway

10 ³ZMT, Leibniz Centre for Tropical Marine Research, Bremen, 28359, Germany

11 ⁴Woods Hole Oceanographic Institution, Geology & Geophysics Department, Woods Hole, 02543, MA, USA

12 ⁵Cell and Plant Physiology Laboratory, CNRS, CEA, INRAE, IRIG, Université Grenoble Alpes, Grenoble, 38054
13 France

14 ⁶Department of Arctic and Marine Biology, UiT, The Arctic University of Norway, Tromsø, 9037, Norway

15 ⁷Université de Nantes, CNRS, Institut des Matériaux Jean Rouxel, IMN, Nantes, 44000 France

16

17 *Correspondence to* Christiane Schmidt christiane.schmidt@leibniz-zmt.de

18

19

20 **Abstract.** Several foraminifera are deposit feeders that consume organic detritus (~~dead particulate~~
21 organic material ~~along~~ with entrained bacteria). However, the role of such foraminifera in the
22 benthic food-web remains understudied. ~~FAs foraminifera may associate with feeding on~~
23 methanotrophic bacteria, which are ^{13}C -depleted, ~~feeding on them has been suggested to may~~ cause
24 negative ~~cytoplasmic and/or calcitic $\delta^{13}\text{C}$ values~~ $\delta^{13}\text{C}$ values in the foraminiferal cytoplasm and/or
25 ~~calcite~~. To test whether the foraminiferal diet includes methanotrophs, we performed a short-term
26 ~~(20-h-d)~~ feeding experiment with *Nonionellina labradorica* from an active Arctic methane-
27 emission site (Storfjordrenna, Barents Sea) using the marine methanotroph *Methyloprofundus*
28 *sedimenti*, and analyzed *N. labradorica* cytology via Transmission Electron microscopy (TEM).
29 We hypothesized that *M. sedimenti* would be visible; ~~post experiment in degradation vacuoles as~~
30 ~~evidenced by their ultrastructure, in degradation vacuoles after this feeding experiment, as~~
31 ~~evidenced by their ultrastructure~~. Sediment grains (mostly clay) occurred inside one or several
32 degradation vacuoles in all foraminifers. In 24% of the specimens from the feeding experiment
33 degradation vacuoles also contained bacteria, although none could be confirmed to be the offered
34 *M. sedimenti*. Observations of the ~~area adjacent to the~~ apertural ~~areae~~ after 20-h incubation
35 revealed three putative methanotrophs, close to clay particles, ~~based on bacterial~~. ~~These~~
36 ~~methanotrophs were identified based on internal-ultrastructural characteristics, such as a type I~~
37 ~~stacked intracytoplasmic membranes (ICM), storage granules (SG) and gram negative cell walls~~
38 ~~(GNCW)~~. ~~Furthermore, more, N. labradorica specimens were examined for specific adaptations~~
39 ~~to this active Arctic methane emission site~~; we noted the absence of bacterial endobionts in all
40 ~~specimens~~ examined *N. labradorica* but confirmed the presence of kleptoplasts, which were often
41 partially degraded. ~~Based on these observations~~ In sum, we suggest that *M. sedimenti* can be
42 consumed ~~by N. labradorica~~ via untargeted grazing in seeps and that *N. labradorica* can be
43 generally classified as a deposit feeder at this Arctic site. ~~These results suggest that if~~
44 ~~methanotrophs are available to the foraminifera in their habitat, their non-selective uptake could~~
45 ~~make a substantial contribution to altering $\delta^{13}\text{C}_{\text{test}}$ values. This in turn may impact metazoans~~
46 ~~grazing on benthic foraminifera by altering their $\delta^{13}\text{C}$ signature.~~

47

48 benthic foraminifera – feeding experiment – grazing - marine methanotrophs – Arctic methane
49 seeps– transmission electron microscopy – ultrastructure – kleptoplasts- protist – molecular
50 identification

51 **1. Introduction**

52 In methane seep sites, the upward migration of methane affects the pore-water chemistry of near-
53 surface sediments, where benthic foraminifera ~~inhabiting the sediment interface have been shown~~
54 ~~to~~ live (e.g. Dessandier et al., 2019). Extremely light isotopic signals of $\delta^{13}\text{C}$ have been measured
55 in seep-associated foraminiferal calcite tests (Wefer et al., 1994; Rathburn et al., 2003; Hill et al.,
56 2004b; Panieri et al., 2014). ~~Studies specifically looking at living (rose bengal stained)~~
57 ~~foraminiferal tests support the hypothesis that the carbon isotopic composition is strongly~~
58 ~~influenced by the porewater DIC (McCorkle et al., 1990a). Interspecific $\delta^{13}\text{C}$ differences between~~
59 ~~species with similar depth indicate sometimes taxon-specific “vital” effects (McCorkle et al.,~~
60 ~~1990a). One Those “vital” effects describe the biology of the different species, which could reflect~~
61 ~~different feeding patterns. It has been suggested that *Nonionella auris* is an indicator of methane~~
62 ~~release and possibly explanation of low $\delta^{13}\text{C}$ signals in foraminifera could be due to the~~
63 ~~ingestion ingests of ^{13}C -depleted methanotrophs oxidizing bacteria (Wefer et al., 1994).~~
64 Recently, ~~specimens of the foraminifer *Melonis barleeanus* (Williamson, 1858) collected from~~
65 ~~an active methane seep site were was found to be~~ closely associated with ~~a~~ putative methanotrophs
66 ~~at their apertural region reasoning the need to examine feeding habits of foraminifera living on or~~
67 ~~around methane seeps (Bernhard and Panieri, 2018), providing impetus to examine feeding habits~~
68 ~~of foraminifera living in or around methane seeps.~~
69 ~~The observation by Bernhard and Panieri (2018) brought to light the need to examine feeding~~
70 ~~habits of foraminifera living on or around methane seeps. The species *M. barleeanus* could feed~~
71 ~~on aerobic methane oxidizing bacteria (methanotrophs), which are abundant in the water column~~
72 ~~around methane seeps (Tavormina et al., 2010). Methanotrophs produce the biomarker diplopterol,~~
73 ~~which has an extremely light $\delta^{13}\text{C}$ signature (-60‰) and makes methanotrophs isotopically very~~
74 ~~light themselves (Hinrichs et al., 2003). If Our hypothesis is that if foraminifera accidentally or~~
75 ~~intentionally ingest methanotrophs, $\delta^{13}\text{C}$ values of foraminiferal cytoplasm should be altered by~~
76 ~~such phagocytosis their diet. However, experimental evidence was inconclusive whether isotope~~
77 ~~labelling of food can influence foraminiferal calcite, as no new calcite was produced during~~
78 ~~experiments using the foraminifera *Haynesina germanica* and *Ammonia beccari* (Mojtabid et al.,~~
79 ~~2011). Experiments using a a novel high-pressure culturing system incubator on *Cibicides*~~
80 ~~*wuellerstorfi* illustrated revealed the difficulty to measure the sensitive relationship between~~
81 methane exposure ~~and the foraminifera *Cibicides wuellerstorfi*. However, it was shown in onethis~~

82 ~~organisms and associated foraminiferal $\delta^{13}\text{C}$ values are the same as in planktonic foraminifera~~
83 (Wollenburg et al., 2015). ~~It is also not yet conclusive if diet can influence foraminiferal calcite,~~
84 ~~as new calcite did not form during experiments (Mojtahid et al., 2011).~~
85 Several studies found that the lightest isotopic $\delta^{13}\text{C}$ values were measured in tests coated by
86 methane-derived authigenic carbonate (MDAC) overgrowth (Torres et al., 2010; Panieri et al.,
87 2014; Consolaro et al., 2015; Panieri et al., 2017; Schneider et al., 2017). MDACs represent a
88 diagenetic alteration of the foraminiferal test that alters the $\delta^{13}\text{C}$ of the foraminiferal isotope record
89 It can form high-Mg calcite coatings contributing to the bulk of foraminiferal carbonate up to 58
90 wt% MgCO (Schneider et al., 2017). MDACs are formed at the SMTZ, the sulfate-methane-
91 transition zone (SMTZ), near the sediment-water interface where the upward flow of methane
92 encounters the downward diffusion of sulfate from overlying seawater (Bian et al., 2001;
93 Schneider et al., 2017).

94 Foraminifera play an important role in the carbon cycle on the deep seafloor (Nomaki et al., 2005)
95 where feeding behavior and food preference vary with species (Nomaki et al., 2006). Selected
96 species of deep-sea benthic foraminifera have been shown to feed selectively on ^{13}C -labeled algae
97 from sedimentary organic matter, but unselectively on ^{13}C -labeled bacteria of the strain *Vibrio*
98 (Nomaki et al., 2006). A study from the seafloor around Adriatic seeps suggested that $\delta^{13}\text{C}$ of
99 foraminiferal cytoplasm could be influenced by feeding on the sulfur-oxidizing bacterium
100 *Beggiatoa*, whose abundance was also positively correlated with foraminiferal densities Panieri,
101 (Panieri, 2006). Generally, some foraminifera can ingest dissolved organic matter (DOM); some
102 are herbivorous, carnivorous, suspension feeders and most commonly deposit feeders ~~reviewed~~
103 ~~in~~ (reviewed in Lipps, 1983). ~~{Goldstein, 1994 #1903}~~ Deposit feeders are omnivorous, gathering
104 fine-grained sediment (e.g., clay) and associated bacteria, organic detritus (dead particulate organic
105 material) and, if present, diatom cells using their pseudopodia. ~~Hence, bacteria are involuntarily~~
106 ~~part of the “food mix” (Levinton, 1989).~~ Based on the ultrastructure of the diet found in vacuoles
107 ~~several species of foraminifera from different habitats have already been classified to be deposit~~
108 ~~feeders~~ (Goldstein and Corliss, 1994).

109 ~~The fact that bacteria are sometimes part of the “food mix” made us~~ Here we investigate if
110 *Nonionellina labradorica* ~~associated would feed in a short-term feeding experiment on the marine~~
111 ~~with-methanotrophs, e.g. *Metyloprofundus sedimenti*, in a short term feeding experiment and~~
112 ~~compare its ultrastructure on experimental specimens and field specimens. —*Nonionellina*~~

Formatted

113 ~~the bivalve *Norionella* from the Arctic region, which was first described by C. H. C. (1991) in the Arctic~~
 114 with *N. digitata* in Svalbard fjord sediments (Hald and Korsun, 1997; Shetye et al., 2011; Fossile
 115 et al., 2020), (Carrier et al., 2020). Next ~~In addition to its wide distribution, it is an especially interesting experimental species~~
 116 ~~for feeding studies~~ because it hosts kleptoplasts, i.e. sequestered chloroplasts, of diatom origin
 117 inside cytoplasm (Cedhagen, 1991; Jaffar et al., 2018) (Cedhagen, 1991; Jaffar et al., 2019b). SEM images of *Norionella labradorica*'s aperture
 118 shows a specific ornamentation, possibly a morphological adaptation to this “predatory” mode of
 119 life for obtaining the kleptoplasts (Bernhard and Bowser, 1999). ~~Denitrification has been~~
 120 ~~speculated for *N. labradorica*~~ (reviewed in Charrieau et al., 2019), ~~because the foraminiferal genus~~
 121 ~~*Norionella* is potentially capable of denitrify, which was demonstrated on two species of *Norionella*, *N. cf. stella* (Risgaard-Petersen et al., 2006,~~
 122 ~~Q. At this site our samples were taken at GHP3, which is referred to as an underwater gas hydrate-bearing mound (Hong~~
 123 degradation vacuoles of this species from an active methane-emitting site in the Arctic
 124 (Storfjordrenna, Barents Sea) ~~before and after a feeding experiment.~~

Field Code Changed

Formatted: Font: Italic

Field Code Changed

Field Code Changed

125 2. Materials and methods

126 2.1. Site description and sampling living foraminifera

127 The sampling site was located app. 50 km south of Svalbard at 382m water depth at the mouth of
 128 Storfjordrenna (Serov et al., 2017). The site is characterized by several large gas hydrate pingos
 129 (GHP), which actively vent methane ~~spread~~ over an area of 2.5 km². ~~Q. At this site our samples~~
 130 ~~were as~~ taken at GHP3, which is referred to as an underwater gas hydrate-bearing mound (Hong
 131 et al., 2017; Hong et al., 2018). GHP3 is a ~500-m diameter, 10-m tall mound that actively vents
 132 methane (Fig. 1). Marine sediment samples were collected during CAGE cruise 18-05 supported
 133 by the research vessel *Kronprins Haakon* ~~en~~ in October 2018 and sampled ~~from the seafloor~~ by
 134 the Remotely Operated Vehicle (ROV) *Ægir*. A blade corer (surface dimensions 27 x 19 cm, Fig.
 135 1c) was used to sample living foraminifera; it was placed directly in the vicinity of bacterial mats.
 136 The blade corer containing the sediment sample was opened immediately once onboard. A small
 137 aquarium hose was used to sample the ~~upper most~~ surface layer (0-1 cm). The ~~wet~~ sediment was
 138 collected in petri dishes and wet sieved to a size range of 250-500 µm, which served as source of
 139 living (cytoplasm containing) foraminifera. The species *N. labradorica*, which was ~~the visibility~~
 140 abundant, was subsequently used for ~~a~~ feeding experiments described in detail below. ~~A previous~~
 141 ~~study on GHP1 in Storfjordrenna also showed also *N. labradorica* is also occurring in other~~
 142 ~~sediment cores (MC_902 and MC_919) in the top 2 cm (Carrier et al., 2020).~~

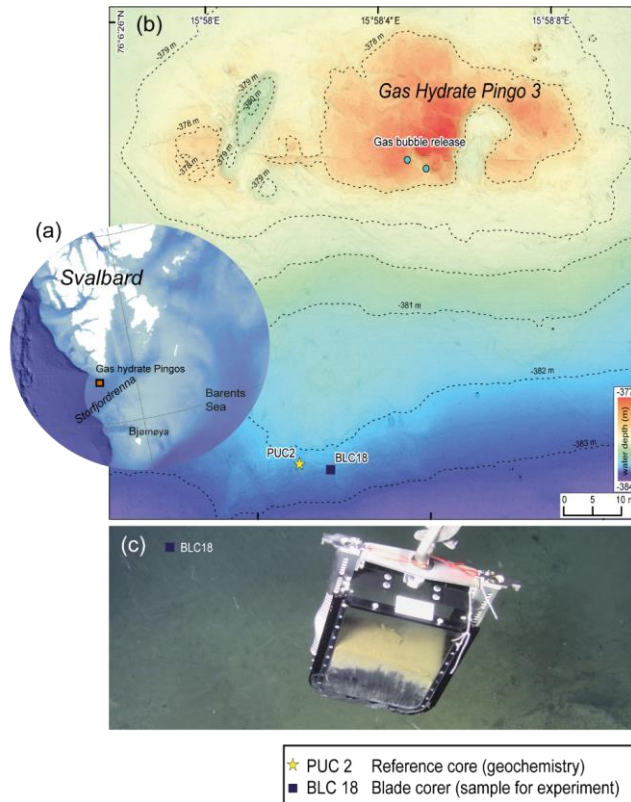


Figure 1. Description of the sampling site Gas Hydrate Pingo 3 (GHP3), a gas-hydrate bearing mound, which actively vents methane, located in Storfjordrenna Barents Sea. (a) Map illustrating Svalbard Archipelago and the distance towards the sampling site, is app. 50 km offshore. (b) Map of sampling site GHP3, active gas bubble release is marked on the top of the underwater mound, yellow star indicates location of push corer PUC2 (taken for geochemical analysis), black squared box indicates the location of the blade corer BLC18 (from which the sediment was derived source for the experiment). (c) Underwater image of retrieval of BLC18 taken by ROV camera of ROV (remotely-operated vehicle) illustrating the coloration of sediment with the sea-floor visible in background.

144 **2.2. Geochemistry of the study site**

145 For geochemical analysis of the study site a push corer (PUC2; henceforth ~~) was used~~ (referred to
146 as geochemistry core) was taken to obtain measurements of ~~fr~~ $\delta^{13}\text{C}_{\text{DIC}}$ and sulfate, ~~because~~ as blade
147 corer (BLC18) did not allow those measurements. PUC2 was taken in close vicinity to BLC18,
148 ~5m apart (see Figure S1 Fig 1). Pore-water samples were taken from PUC2 using rhizons that
149 were inserted through pre-drilled holes in the core tube at intervals of 1 cm (Table S1). Acid
150 washed 20-ml syringes were attached to the rhizons for pore water collection. Depending on the
151 amount of pore water collected, the samples were split for $\delta^{13}\text{C}_{\text{DIC}}$ and sulfate measurements. To
152 the samples, 10 μL of saturated HgCl_2 (aqueous) was added to stop microbial activity, and stored
153 in cold conditions (5°C). ~~$\delta^{13}\text{C}_{\text{DIC}}$ was determined using a~~ ThermoScientific Gasbench II coupled
154 to a ThermoScientific MAT 253 IRMS at the Stable Isotope Laboratory (SIL) at CAGE, UiT was
155 used to determine $\delta^{13}\text{C}_{\text{DIC}}$ of the pore-water. Anhydrous phosphoric acid was added to small glass
156 vials (volume 4.5 mL), that were closed and flushed with helium 5.0 gas before the pore-water
157 sub-sample was measured. A pore-water sub-sample (volume 0.5 mL) was then added through the
158 septa with a syringe needle, followed by equilibration for 24 h at 24°C to liberate the CO_2 gas.
159 Three solid calcite standards with a range of +2 to -49 ‰ were used for normalization to $\delta^{13}\text{C}$ -
160 VPDB. Correction of measured $\delta^{13}\text{C}$ by -0.1 ‰, was done to account for fractionation between
161 (gas) and (aqueous) in sample vials. Instrument precision for $\delta^{13}\text{C}$ on a MAT253 IRMS was ~~+/-~~
162 +/- 0.1 ‰ (SD). Sulfate was measured with a Metrohm ion chromatography instrument equipped
163 with column Metrosep A sup 4, and eluted with 1.8 mmol/L Na_2CO_3 + 1.7 mmol/L NaHCO_3 at
164 the University of Bergen.

165 **2.3. Culturing of the marine methanotroph *M. sedimenti***

166 *Methyloprofundus sedimenti* PKF-14 had been previously isolated from a water-column sample
167 collected at Prins Karls Forland, Svalbard in the laboratory at UiT in Tromsø. *Methyloprofundus*
168 *sedimenti* were cultured in 10-ml batches of a 35:65 mix of 1/10 Nitrate Mineral Salt medium
169 (NMS) and sterile filtered sea water using 125-mL Wheaton® serum bottles with butyl septa and
170 aluminum crimp caps (Teknolab®). Methane was injected to give a headspace of 20% methane in
171 air, and the bottles were incubated without shaking at 15°C in darkness. Purity of the cultures and
172 cell integrity was verified by microscopy and by absence of growth on agar plates with a general
173 medium for heterotrophic bacteria (tryptone, yeast extract, glucose and agar).

174 ~~Transmission Electron Microscopy was performed on culture aliquots to allow morphological~~
175 ~~comparison to previously published work (Tavormina et al., 2015). *Methyloprofundus sedimenti*~~
176 ~~strain PKF 14 cells have a gram negative cell wall, coccoid to slightly elongated shape and~~
177 ~~characteristic stacked intracytoplasmic membrane (ISM) and storage granules (SG) (Fig 2e).~~
178 ~~Additionally, 16S rRNA gene sequencing was performed (data not shown) to confirm it to be~~
179 ~~similar to the published *Methyloprofundus sedimenti* (Tavormina et al., 2015).~~

180 On the ship, *Nonionellina labradorica* (Fig. 2a,b) specimens showing a dark greenish brown
181 cytoplasm were picked using sable artist brushes under a stereomicroscope immediately after wet
182 sieving the sediment using natural seawater delivered from the ship pump. Living specimens had
183 a partly inorganic covering surrounding the test, which was gently removed using fine artist
184 brushes. Those so-called cysts are nothing unusual with many foraminiferan taxa (Heinz et al.,
185 2005). ~~Another Nonionellidae, *Nonionella iridea*, was similarly embedded with a cyst / covering~~
186 ~~in sediment~~

187 Our specimens were subsequently rinsed twice in filtered artificial seawater to remove any
188 sediment before placing them into the experimental petri dishes. Care was taken that those were
189 minimally exposed to light during preparation of the experiment, as kleptoplasts are known to be
190 highly light sensitive in this foraminifer (Jaufrais et al., 2019b).

191 The experiment with *M. sedimenti* was conducted for a total duration of 20-h to resemble
192 previous experiments on *N. labradorica* using transmission electron microscopy and
193 nanometre-scale secondary ion mass spectrometry isotopic imaging (TEM-NanoSIMS) (Jaufrais
194 et al., 2019b) (Jaufrais et al., 2019), and included two more time points at 4 and 8 h, where
195 incubations were terminated. A short pre-experimental phase (2-4 h) was included before the initial
196 start of the feeding experiment, to allow specimens to acclimate. During the pre-experimental
197 phase specimens were not fed and resided in the petri dishes to adjust to the experimental
198 conditions. The 20 h feeding experiment with *M. sedimenti* started after a short starvation phase
199 where organisms resided in petri dishes with ASW for 2-4 h and were not fed or manipulated
200 during this time. The feeding experiment consisted of several small petri dishes (3.5 cm Ø, 3 mL)
201 each containing five foraminifera *N. labradorica* in ASW at ambient salinity 35 (Red Sea Salt).
202 Petri dishes were sealed with Parafilm® and covered with aluminum foil and placed inside the
203 incubator in complete darkness. Temperature inside the chamber was maintained at 2-3°C, which
204 is within the range of the site's bottom-water temperature (-1.8 – 4.6°C) (Hong et al., 2017). The

205 feeding of *M. sedimenti* was performed once at the beginning of the experiment by adding 100 μ L
 206 of culture to 3 mL of artificial seawater to produce a final concentration of $\sim 1 \times 10^6$ bacteria / mL
 207 in ~~each petri dish~~ the experiment. Previously conducted feeding studies were used as guides:
 208 Muller and Lee (1969) used 1×10^4 bacteria/mL seawater and Mojtahid et al. (2011) used 4×10^8
 209 bacteria/mL seawater.
 210 Five foraminifera, which served as initial/field specimens (Table 1), ~~–~~ were fixed without *M.*
 211 *sedimenti* incubation. The respective petri dishes, were incubated for 4, 8 and 20 h to determine if
 212 incubation duration influenced response of the foraminifera to the methanotroph. One petri dish
 213 containing five foraminifera, which were un-fed and fixed at 20 h, served as a negative “control”.
 214 After the end of the respective incubation times, each foraminifer was picked with a sterilized fine
 215 artist brush, which was cleaned in 70% ethanol between each specimen, and placed individually
 216 into a fixative solution (4% glutaraldehyde and 2% paraformaldehyde dissolved in ASW).

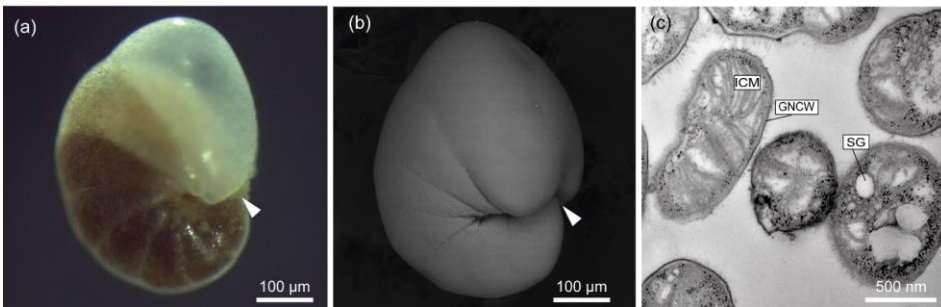


Figure 2 Exemplary illustration of *Nonionellina labradorica*, utilized in this study. (a) Reflected light microscopy image from a specimen directly after sampling, white arrowhead indicates aperture location. (b) Scanning electron image from a specimen before molecular analysis was performed, white arrowhead indicates aperture location. (c) Transmission electron microscopy image of a culture of *Methyloprofundus sedimenti*, the marine methanotroph used in the feeding experiment. The characteristic features for methanotroph identification include is the typical type I ICM=intracytoplasmic membranes (ICM). Furthermore, other internal structures visible are, SG=storage granules (SG), and a GNCW=gram-negative cell wall (GNCW).

217 2.5. Transmission Electron microscopy (TEM) preparation

218 Samples of *N. labradorica* preserved in fixative solution were transported to the University of
 219 Angers, where they were prepared for ultrastructural analysis using established protocols
 220 (Lekieffre et al., 2018). Four embedded foraminiferal cells per treatment Embedded foraminiferal
 221 cells were sectioned using an ultramicrotome (Leica® Ultracut S) equipped with a diamond knife

222 (Diatome[®], ultra 45°). Grids were stained using UranylLess[®] EM Stain (EMS, USA). Ultra-thin
223 sections (70 nm) were observed with a JEOL JEM-1400 TEM at the SCIAM facility, University
224 of Angers.

225 To document the ultrastructure of *Methyloprofundus sedimenti*, a sub-sample of the culture used
226 for experiments was imaged with TEM (Fig. 2c). To do so, an exponentially growing culture was
227 collected, centrifuged, pre-fixed with 2.5 % (w/v) glutaraldehyde in growth medium overnight,
228 washed in PBS (Phosphate Buffered Saline), then post fixed with 1% (w/v) aqueous osmium
229 tetroxide for 1.-5 hours at room temperature. After dehydration in an ethanol series, the samples
230 were embedded in an Epon equivalent (Serva) epoxy resin. Ultra-thin sections were cut on a Leica
231 EM UC6 ultramicrotome, and stained with 3 % (w/v) aqueous uranyl acetate followed by staining
232 with lead citrate (Reynolds, 1963) at 20 °C for 4–5 min. The samples were examined with a JEOL
233 JEM-1010 transmission electron microscope at an accelerating voltage of 80 kV with a Morada
234 camera system at the Advanced Microscopy Core Facility (AMCF), Faculty of Health Science,
235 UiT The Arctic University of Norway.

236 2.6. Foraminifera ultrastructural observation and image processing

237 Four specimens per experimental time point (initials, 4, 8 and -20 h) plus one un-fed (control)
238 specimen were examined with the TEM. From each specimen, a minimum of 50 TEM images was
239 taken, including images detailing the degradation vacuoles (5-27 images of degradation vacuoles
240 per specimen). The ultrastructure was examined at different parts of the images-sections focusing
241 (a) in the cell interior to document vitality, (b) on degradation vacuoles to determine their content,
242 and (c) at the exterior to survey for microbes entrained in remnant “reticulopodial trunk” material,
243 ~~which can be extended outside foraminiferal tests during feeding and locomotion (Anderson and~~
244 ~~Le9) has a high resolution TEM and PACFA-EDC and XDO for image processing and data analysis.~~

245 2.7. Molecular genetics and morphology

246 DNA metabarcoding and morphological documentation were performed on 13 specimens of *N.*
247 *labradorica*. Briefly, live specimens were dried on micropaleontological slides and transported in
248 a small container, cooled with ice-pads to the University of Angers. All specimens were imaged
249 for morphological analysis using a Scanning Electron Microscope (SEM; EVOLS10, ZEISS, Fig.
250 S1) followed by individually extracting total DNA in DOC buffer (Pawlowski, 2000). To amplify
251 foraminiferal DNA, a hot start PCR (2 min. at 95°C) was performed in a volume of 25µl with 40

252 cycles of 30 s at 95°C, 30 s at 50°C and 2 min at 72°C, followed by 10 min at 72°C for final
253 extension. Primers s14F3 and sB were used for the first PCR and 30 cycles at an annealing
254 temperature of 52°C (other parameters unchanged) for the nested PCR with primers s14F1 and J2
255 (Pawlowski, 2000; Darling et al., 2016). Positive amplifications were sequenced directly with the
256 Sanger method at Eurofins Genomics (Cologne, Germany). For taxonomic identification, DNA
257 sequences were compared first with BLAST (Basic Local Alignment Search Tool) (Altschul et al.,
258 1997) and then within an alignment comprising other Nonionids implemented in SeaView (Gouy
259 et al., 2010) and corrected manually.

260 3. Results

261 3.1. Sample description and geochemistry of the study site

262 The visual observation of the sediments within the blade corer BLC18 immediately after sampling
263 (Fig. 1c) indicated that the sediment appeared light grey – yellowish in the upper part until app.
264 13 cm and dark brown from app. 13 cm to the bottom. ~~At approximately 13 cm~~ the sulfate
265 measured in the pore water of the geochemistry core (PUC2) declined from ~2750 ppm at the
266 sediment-water interface to ~706 ppm ~~at approximately 13 cm (see Fig. S1, Table S1)~~. A decline
267 in sulfate concentration indicates that the anaerobic oxidation of methane (AOM) occurred at app.
268 13 cm depth. The SMTZ (Sulfate Methane Transition Zone) characterized by ~~a reduced $\delta^{13}\text{C}$~~
269 ~~DIC value of~~ -32‰ at app. 13 cm sediment depth can be considered shallow on the global average
270 (Egger et al., 2018).

271 3.2. Ultrastructure of methanotroph culture used in the feeding experiment

272 ~~Transmission Electron Microscopy was performed on culture aliquots to allow morphological~~
273 ~~comparison to previously published work (Tavormina et al., 2015). *Methyloprofundus sedimenti*~~
274 ~~strain PKF-14 cells are coccoid to slightly elongated shape and is characterized by typical type I~~
275 ~~strains (CMF2) *Methyloprofundus sedimenti* by typical type I strains (CMF2) with a~~
276 ~~negative cell wall (GNCW), which are not uniquely characteristic of methanotrophs (GNCW) (Fig. 2c).~~
277 ~~Additionally, 16S rRNA gene sequencing was performed (data not shown) to confirm it to be~~
278 ~~similar to the published *Methyloprofundus sedimenti* (Tavormina et al., 2015). These features were used to identify *M. sedimenti*.~~

Formatted

279 **3.3. Foraminiferal ultrastructure from an Arctic seep environment**

280 **3.3.1 General ultrastructure**

281 All 17 specimens examined for ultrastructure were considered living at the time of observation
282 (Fig. 3), as the mitochondria had characteristic double membranes and occasionally visible cristae
283 (Nomaki et al., 2016). Cytoplasm exhibited several vacuoles and kleptoplasts concentrated in the
284 youngest chambers (Fig. 3a) and, in some specimens, ~~the a~~ nucleus with nucleoli was visible (Fig.
285 3b). Kleptoplasts were numerous throughout the cytoplasm and occurred in the form of a single
286 chloroplast (Fig. 3a-b), or as double chloroplasts (Fig. S2a-d). Not all kleptoplasts were intact;
287 some showed peripheral degradation of the membranes indicated by an increasing number of white
288 areas between pyrenoid, lamella and thylakoids (Fig. S2a-d). The mitochondria occurred often in
289 small clusters of two to five throughout the cytoplasm and were oval, round or kidney-shaped in
290 cross section (Fig. 3e-f). Peroxisomes in *N. labradorica* occurred mostly as pairs (Fig. 3c) or small
291 clusters of 3-4 spherical organelles (Fig. S3a+b). ~~The mitochondria occurred often in small~~
292 ~~clusters of two to five throughout the cytoplasm and were oval, round or kidney shaped in cross~~
293 ~~section (Fig. 3e-f).~~ Sometimes, but not always, peroxisomes were associated with endoplasmic
294 reticulum (Fig. S3b-e) but could also occur alone. Golgi apparatus (Fig 3d) had intact membranes,
295 often occurring near mitochondria.

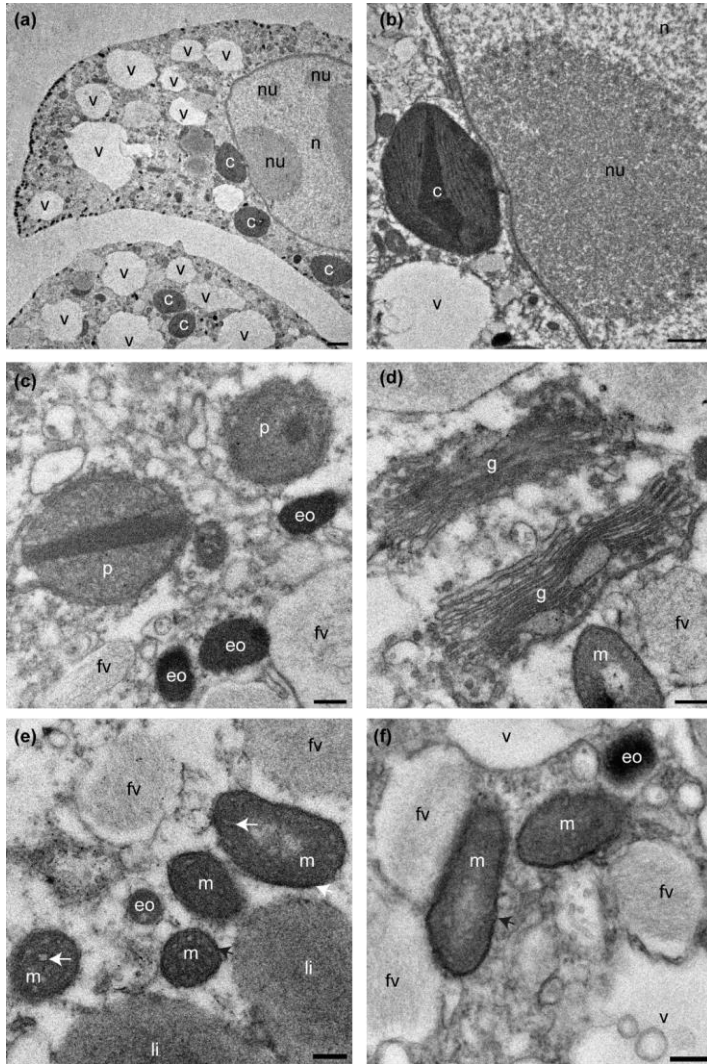


Figure 3 Transmission electron micrographs showing cellular ultrastructure of *N. Labradorica*. (a) Cytoplasm showing parts of two chambers, with nucleus with nucleoli, vacuoles and several kleptoplasts, (b) nuclear envelope, nucleoli, and kleptoplasts, (c) peroxisomes and electron opaque bodies, (d) Golgi, (e-f) mitochondria. V=vacuole, c=kleptoplast, nu=nucleoli, n=nucleus p=peroxisome, eo=electron opaque body, m=mitochondrion, fv=fibrillar vesicle, li=lipid droplet. Scales: (a) 2 μ m, (b) 1 μ m, (c-f) 200 nm

297 **3.3.2 Ultrastructure of aperture-associated bacteria**

298 In total, three putative methanotrophs were identified in the vicinity of two ~~foraminifer~~ specimens
299 (sample E39, Fig. 4; E37, Fig. 5). ~~These microbes~~ were identified ~~adjacent next~~ to reticulopodial
300 remains ~~in the cross-section~~ (Fig. 4b). As an aid for identification of *M. sedimenti* we used the
301 characteristics shown in the literature (~~Tavormina~~ (Tavormina et al., 2015) ~~et al. 2015~~) and ~~a~~ our
302 own TEM observation obtained from *M. sedimenti* culture (Fig. 2c). As noted, *Methyloprofundus*
303 *sedimenti* is characterized by a typical type I intracellular ~~stacked~~ cytoplasmic stacked membrane
304 (ISSM). ~~Other characteristics, which are not specific for methanotrophs, were included~~ storage
305 granules (SG) and a typical gram-negative cell wall (GNCW) (Fig. 2c). On specimen E39 from
306 the 20 h treatment, we found the methanotroph exhibiting the clearest internal structure, having
307 both typical type I ~~stacked~~ intracytoplasmic stacked membranes (ISCM and +SG) and ~~a second~~
308 ~~putative methanotroph showing SG+GNCW~~ (Fig. 4c). ~~Specimen E36, from the 20 h treatment,~~
309 ~~hosted another putative methanotroph showing three large SG (Fig. 5). Storage granules occur~~
310 ~~through this putative methanotroph (Fig. 5c).~~

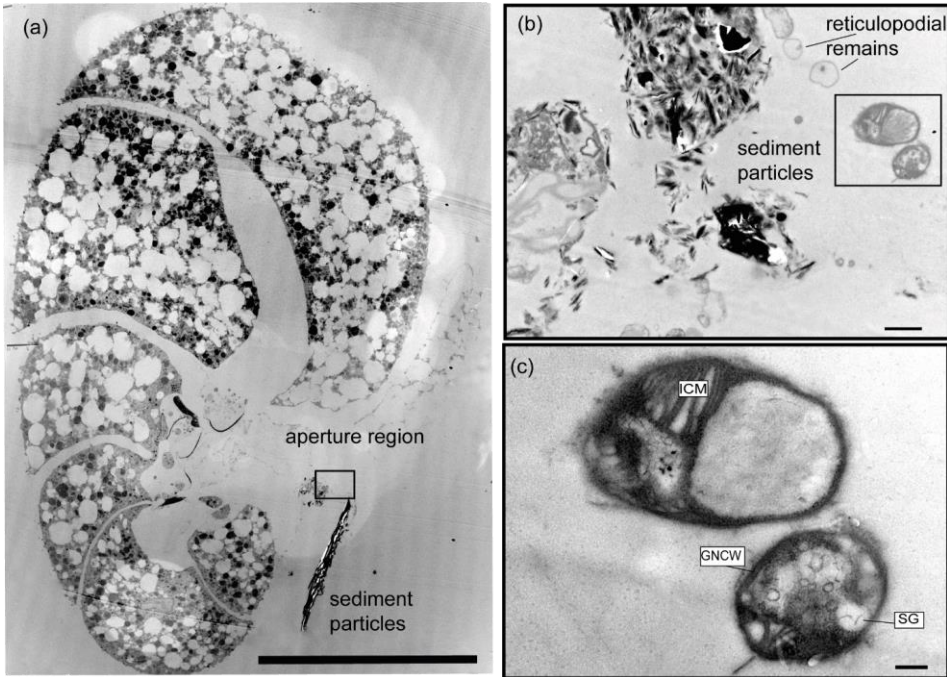
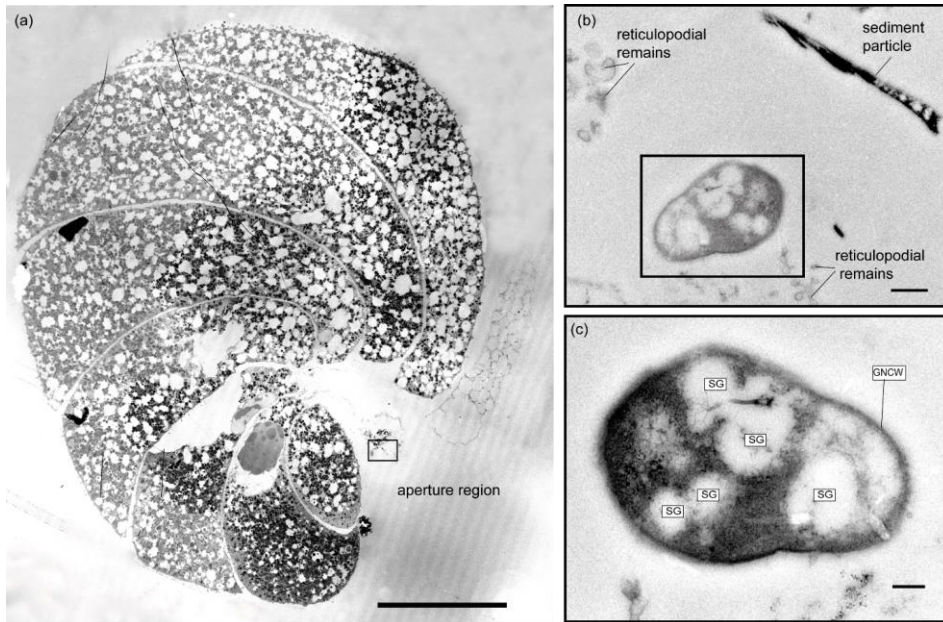


Figure 4 Transmission electron micrographs of *N. labradorica* from 20 h treatment (sample E39) (a) Stitched cross section of TEM images showing location of methanotroph at the aperture region (black rectangle is the location of image shown in panel b) (b) Location of two putative methanotrophs next to sediment particles and putative reticulopodial remains (black rectangle is location of image shown in panel c) (c) Close up of two putative methanotrophs revealing detailed feature for identification, such as typical type I stacked intracytoplasmic stacked-membranes (ICM), and other characteristics, such as storage granules (SG), and gram-negative cell wall (GNCW), scale bars: a: 100 μm, b: 1 μm, c: 200 nm.



312

Figure 5 Transmission electron micrographs of *N. labradorica* from 20 h treatment (sample E37) (a) Stitched cross section of TEM images showing location of putative methanotroph (black rectangle) at the aperture region. (b) Location of the putative methanotroph next to sediment particles and sections of the putative reticulopodial remains (c) Close up of putative methanotroph showing several SG throughout its cell, scale bars: a: 100 μm , b: 0.5 μm , c: 200 nm.

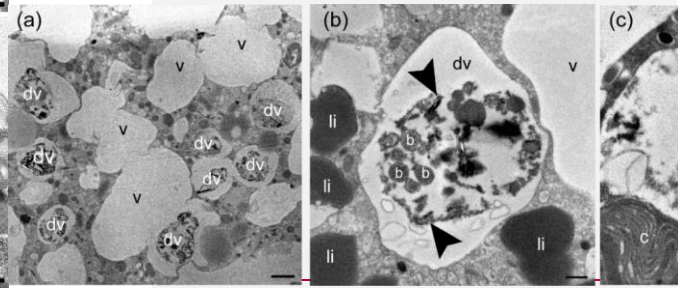
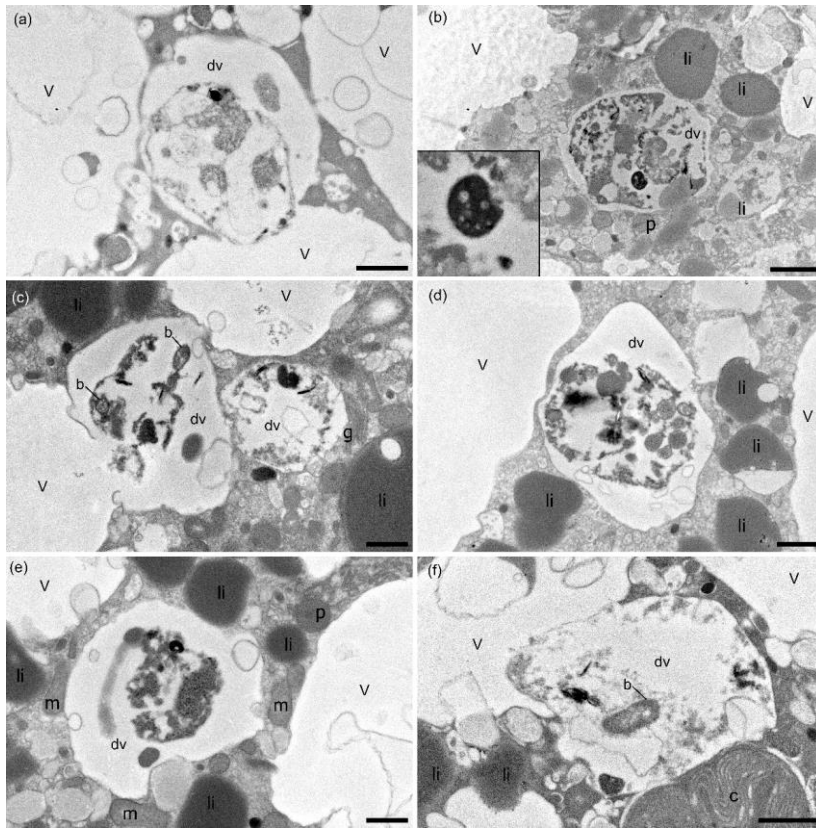
313

314 3.3.3 Contents of degradation vacuoles

315 Digestive vacuoles and food vacuoles are often summarized as degradation vacuoles in the
 316 literature (Lekieffre et al., 2018) and this makes sense for our study as well. A degradation vacuole
 317 is a vacuole where enzymatic activities degrade contents, often making them unidentifiable (Bé et
 318 al., 1982; Hemleben et al., 2012). Sediment particles were present in many degradation vacuoles.

319 The sediment grains ~~were~~ are easy to recognize in the TEM image as angular grains ~~spiking out of~~
 320 inside the vacuoles, next to organic debris, which can have many different shapes. Each specimen
 321 had at least one degradation vacuole and mostly several, which were ~~degradation vacuole filled~~
 322 with sediment particles present (Table 1). If a sediment particle was visible, the vacuole was
 323 defined as a degradation vacuole (dv), and if it was not and empty then it was defined as a standard
 324 vacuole (v) (Fig. 6). The observed entrained sSediment particles were platelets, are likely the
 325 remains of clay grains from the seafloor, and hence show that the vacuole must contain ell foreign

326 objects, around which degradation processes have started. Next to sediment particles, Four out of
 327 17 specimens examined (23%) had one or more a few bacteria of various sizes inside their degradation
 328 vacuoles next to sediment particles. (Fig 6 c, f b-e).



329

Figure 6 TEM micrographs of *N. labradorica* showing degradation vacuoles containing miscellaneous items, including bacteria (b), inorganics (clay platelets) and unidentifiable remains after 4h incubation, which are shown enlarged in the left side of the image in a zoom window (a,b; specimens E27, E28, respectively); after 8h incubation (c,d; specimen E14), after 20h incubation (e,f; specimens E36, E37, respectively). v=vacuole, dv=degradation vacuole, c=kleptoplast, p=peroxisome, m=mitochondrion, li=lipid, g= Golgi. Scales: (a, c-f) 1 μ m, (b) 2 μ m. TEM-micrographs of *N. labradorica*. (a) Overview of degradation vacuoles (dv) in relation to empty vacuoles (v) in the youngest chambers of specimen E5 (field). (b) Bacteria in degradation vacuoles (white b) next to clay particles (black arrow) in specimen E14 (8 h incubation). (c) Elongated bacterium inside degradation vacuole adjacent to clay particles of specimen E37 (20 h incubation), scale bars: a: 2 μ m, b,e: 0.5 μ m.

330 3.4. Foraminiferal genetics

331 Six of 13 specimens analyzed for genetics were positively amplified and sequenced (Fig. S43).
332 The sequences are deposited in GenBank under the accession numbers MN514777 to MN514782.
333 When comparing them via BLAST, they were between 98.6% and 99.6% identical to published
334 sequences belonging to foraminifera identified as the morphospecies *N. labradorica*, from the
335 Skagerrak, Svalbard and the White Sea (Holzmann and Pawlowski, 2017; Jauffrais et al., 2019b).
336 Sequences were also included in an alignment comprising other nonionids implemented in
337 Seaview (not shown) and corrected manually to check the BLAST search. This step confirmed the
338 BLAST identification.

339 4. Discussion

340 4.1. Sampling site and geochemistry

341 The sampling site of blade corer BLC18 was in close proximity (~50 m) to an active methane-vent
342 releasing methane bubbles at the gas hydrate pPingo (GHP3) (Serov et al., 2017). At such sites
343 with high methane fluxes, the SMTZ (sulfate methane transition zone) is shallow, as sulfate ~~in from~~
344 the sediment is readily consumed in the first tens of centimeters (Barnes and Goldberg, 1976;
345 Iversen and Jørgensen, 1993) by sulfate-reducing bacteria (SRB) (reviewed in Carrier et al., 2020).
346 Geochemical analysis of PUC2, revealed an SMTZ at app. 13 cm, ~~which. The depth of 13 cm~~ is
347 rather shallow (Egger et al., 2018), as it can also be several meters deep in other sites (reviewed in
348 Panieri et al., 2017). ~~Similar g~~Geochemical characteristics can be considered ~~similar~~
349 at the sampling location of living specimens (BLC18) ~~given the close proximity of the two locations and~~
350 ~~the core taken for geochemistry (PUC2). The geochemical data at PUC2 allows us conclude that~~
351 ~~the site, where living foraminifera were collected, can be classified as an active methane emission~~
352 ~~site.~~

353

354 4.2. ~~Possible a~~Association ~~sociation~~ with putative methanotrophs

355 The ~~possible~~ association of *N. labradorica* with ~~the three putative~~ methanotrophs ~~could be was~~
356 ~~identified~~ ~~documented~~ via presence of two putative methanotrophs, based on microbial
357 ~~ultrastructure foron two foraminifera specimens based on comparing internal bacterial~~
358 ~~characteristics to published literature~~ (Tavormina et al., 2015). ~~Transmission electron microscopy~~

Formatted: Font: Italic

359 ~~is possible to observe the structure of the family plan. That is, the ratio of the post- and pre- and the post- and pre- of the~~
360 ~~feeding in the experiment. However, there is a small possibility that the associated methanotrophs were not the same as the~~
361 ~~field-remains, to preserve its microbiome. Another benthic foraminifer, *Melonis barleeanus*, has been noted to have clumps of~~
362 ~~putative methanotrophs at the apertural opening of field-collected specimens. Our are similar to field-collected (Bernhard and~~
363 ~~Prüfer 2015) and the methanotrophs of *N. labradorica* have been found to be similar to those of *N. labradorica* and that *N. labradorica*~~
364 ~~described in this study for this species for the first time, shows that methanotrophs may be are ingested via~~
365 ~~untargeted grazing in seeps, as *N. labradorica* appears to be a non-selective feeder.~~

366 **4.3. Feeding on other bacteria and contents of Ddegradation vacuoles show large number of** 367 **sediment particles and few bacteria**

368 Our results of the feeding experiment ~~and experimental specimens~~ show that ~~only~~ 23% of the
369 examined *N. labradorica* specimens contained bacteria inside their degradation vacuoles. That is
370 not a large ~~quantity-proportion~~ compared to ~~presence of~~ sediment particles, which occurred in
371 100% of the examined ~~degradation vacuoles foraminifers~~. ~~From this result, however, we~~ We infer
372 that *N. labradorica* at this site is a deposit feeder, feeding on organic detritus and associated
373 bacteria. The bacteria observed in the degradation vacuoles resembled those from other deep-sea
374 foraminifera (*Globobulimina pacifica* and *Uvigerina peregrina*) and the shallow-dwelling genus
375 *Ammonia* (Goldstein and Corliss, 1994). Salt-marsh foraminifera also feed on bacteria and
376 detritus, as observed in TEM studies (Frail-Gauthier et al., 2019). Scavenging on bacteria has also
377 been observed by other foraminifera from intertidal environments such as *Ammonia tepida* or
378 *Haynesina germanica* (Pascal et al., 2008) and is a logical consequence from detritus feeding.
379 Certain foraminifera have been shown to selectively ingest algae/bacteria according to strain (Lee
380 et al., 1966; Lee and Muller, 1973). From laboratory cultures we know that several foraminifera
381 cultures require bacteria to reproduce, as antibiotics inhibited reproduction (Muller and Lee, 1969).
382 Future studies will need to employ additional~~ly~~ molecular tools to ~~additionally~~ determine the food
383 contents inside the cytoplasm (~~e.g.~~ (e.g. Salonen et al., 2019). ~~For example, aA~~ recent study ~~by~~
384 used metabarcoding to assess the contribution of ~~baeterial-eukaryotic~~ OTUs associated with
385 intertidal foraminifera, ~~and~~ reveal~~inged~~ that *Ammonia* sp. T6 ~~preys on metazoans, ean predate on~~
386 ~~metazoan taxa~~, whereas *Elphidium* sp. S5 and *Haynesina* sp. S16 ~~were~~ are more likely to ingest
387 diatom~~sa~~ (Chronopoulou et al., 2019).

388 **4.4. General ultrastructure of *N. labradorica* collected in a seep environment**

389 Our observations also included the intact nature of all major organelle types of this species, as this
390 was essential to conclude vitality after the experiment (Nomaki et al., 2016). Mitochondria and
391 kleptoplasts were generally homogeneously distributed throughout the cytoplasm confirming
392 previous observations of six *N. labradorica* from the Gullmar Fjord (Lekieffre et al., 2018;
393 Jauffrais et al., 2019b). If mitochondria are concentrated predominately under pore plugs, it can
394 be an indicator that the electron acceptor oxygen is scarce in their environment, as the pores are
395 the direct connection from the cell to the environment. This has been observed in several other
396 studies where mitochondria were accumulated under pores in *N. stella* (Leutenegger and Hansen,
397 1979) and *Bolivina pacifica* (Bernhard et al., 2010).

398 ~~For the specimens samples from our particular site, we also observed kleptoplasts abundantly and~~
399 ~~evenly distributed throughout the cytoplasm, confirming previous TEM studies on the species from~~
400 ~~fjord sediments (Cedhagen, 1991; Jauffrais et al., 2018). Occasionally, Even though our study did~~
401 ~~not focus on kleptoplasts, we could observe that kleptoplasts -were occasionally degraded, which~~
402 ~~could have happened; a) during sampling, b) due to exposure to microscope lights or c) due to the~~
403 ~~age and condition of kleptoplasts inside the host. Kleptoplasts in N. labradorica have been studied~~
404 ~~in detail describing their diatom origin (Cedhagen, 1991), sensitivity to light and missing~~
405 ~~photosynthetic functionality (e.g. (Jauffrais et al., 2019b). (Jauffrais et al., 2019a) It has been~~
406 ~~suggested that kleptoplasts could function as a seasonal energy reservoir, for example, (e.g. in~~
407 ~~winter) (Jauffrais et al., 2016).~~

Formatted: Font: Italic,

408 5. Conclusions

409 Based on the content of degradation vacuoles ~~observed~~, we conclude that *N. labradorica* from
410 GHP3 our study site, an active methane emitting site in the Barents Sea, is a deposit-feeder, as
411 it ingests large amounts of sediment particles together with bacteria as part of consuming detritus
412 detrivorous diet living on the sea floor. On two specimens of the feeding experiment, putative
413 methanotrophs were observed near the N. labradorica aperture, suggesting ingestion of M.
414 sedimenti ~~At the aperture region of two different foraminifera specimens, next to reticulopodial~~
415 ~~remains and sediment particles, we observed three putative marine methanotrophs after 20 h~~
416 ~~incubation. One of the putative methanotrophs had characteristic ISM, which resemble the~~
417 ~~methanotroph M. sedimenti in culture. We conclude that it is possible that N. labradorica may~~
418 ~~ingests M. sedimenti via “untargeted grazing” in this seep sites.~~ Further studies are needed on
419 feeding strategies of several other paleo-oceanographically relevant foraminifera to detangle the

420 relationship between $\delta^{13}\text{C}$ measured in ~~of~~ foraminiferal calcite, ~~their~~ cytoplasm and ~~dietary composition~~ [contribution to their diet](#).

421 **6. Data availability**

422 Data in form of TEM images will be deposited at PANGAEA (~~under~~-doi:

423 Molecular data ~~will be~~ is deposited ~~before publication~~ at Genbank.

424 **7. Sample availability**

425 Samples are available upon request and TEM thinsections archived at the University of Angers.

426 **8. Acknowledgments**

427 We thank the captains, crew members and scientists onboard R/V *Kronprins Haakon* and ROV
428 *Ægir* Team for their assistance; Anne-Grethe Hestnes for growing the methanotroph culture.
429 Florence Manero, Romain Mallet and Rodolphe Perrot at the SCIAM microscopy facility
430 University of Angers are to thank for their expertise with the TEM and SEM. We thank Sunil
431 Vadakkepuliambatta for helping to prepare the map presented in Figure 1; Sophie Quinchar
432 (LPG-BIAF) for supporting the molecular analysis. Funding was received through the Research
433 Council of Norway, CAGE (Center for Excellence in Arctic Gas Hydrate Environment and
434 Climate, project number 223259) and NORCRUST (project number 255150) to GP, EG, and CS.
435 CS position was funded through the MOPGA (Make Our Planet Great Again) fellowship by
436 CAMPUS France, the NORCRUST project and the University of Angers. JMB was partially
437 supported by US NSF 1634469, WHOI's Investment in Science Program, and by the Région Pays
438 de la Loire through the FRESCO Project.

439 **Author Contributions**

440 Designed the project and experiment: GP, EG, CS; Collected samples: CS, EG; Performed
441 experiment: CS; Sample preparation: CS, HR; TEM observations and interpretations: CS, JMB,
442 EG, CL; Conducted molecular genetics: MSc; Wrote the paper: CS, GP, JMB; Provided critical
443 review and edits to the manuscript: EG, CL, MSv, MSc, HR; Contributed
444 reagents/materials/analysis tools: MSv, MSc, CL.

445

446 **Table I.** Summary of TEM observations of *Nonionellina labradorica* comparing field specimens
 447 and experimental specimens. Field specimens (initials) were not fed, nor was a non-fed control
 448 preserved after a 20 h incubation. The only putative methanotrophs were observed and imaged in
 449 specimens from the 20 h incubation. Bacteria of unknown origin were described as rod shaped
 450 cells in the degradation vacuoles.

451

Duration of experiment (h)/field samples	Food provided (yes (x)/no)	Sample ID	Cytoplasm: Degradation vacuole Contents		Aperture region: (putative) Methanotrophs
			bacteria	Clay/in-organics	
Field samples (Initials)	No	E1	no	x	no
	No	E3	no	x	no
	No	E5	no	x	no
	No	E6	no	x	no
4	x	E25	no	x	no
	x	E27	x	x	no
	x	E28	no	x	no
	x	E29	no	x	no
8	x	E14	x	x	no
	x	E15	no	x	no
	x	E16	no	x	no
	x	E17	no	x	no
20	x	E36	x	x	1 x
	x	E37	x	x	no
	x	E38	no	x	no
	x	E39	no	x	2 x
Control (20)	no	E44	no	x	no

452

453

454

455 **References-:**

456

457 Altschul, S. F., Madden, T. L., Schäffer, A. A., Zhang, J., Zhang, Z., Miller, W., and Lipman, D.
458 J.: Gapped BLAST and PSI-BLAST: a new generation of protein database search programs,
459 Nucleic Acids Res., 25, 3389-3402, <https://doi.org/10.1093/nar/25.17.3389>, 1997.

460 Barnes, R. O. and Goldberg, E. D.: Methane production and consumption in anoxic marine
461 sediments, Geology, 4, 297-300, [https://doi.org/10.1130/0091-
462 7613\(1976\)4<297:MPACIA>2.0.CO;2](https://doi.org/10.1130/0091-7613(1976)4<297:MPACIA>2.0.CO;2), 1976.

463 Bé, A. W. H., Spero, H. J., and Anderson, O. R.: Effects of symbiont elimination and reinfection
464 on the life processes of the planktonic foraminifer Globigerinoides sacculifer, Marine Biology,
465 70, 73-86, <https://doi.org/10.1007/BF00397298>, 1982.

466 Bernhard, J. M. and Bowser, S. S.: Benthic foraminifera of dysoxic sediments: chloroplast
467 sequestration and functional morphology, Earth-Sci. Rev., 46, 149-165,
468 [https://doi.org/10.1016/s0012-8252\(99\)00017-3](https://doi.org/10.1016/s0012-8252(99)00017-3), 1999.

469 Bernhard, J. M. and Panieri, G.: Keystone Arctic paleoceanographic proxy association with
470 putative methanotrophic bacteria, Sci Rep-Uk, 8, 10610, [https://doi.org/10.1038/s41598-018-
471 28871-3](https://doi.org/10.1038/s41598-018-28871-3), 2018.

472 Bernhard, J. M., Goldstein, S. T., and Bowser, S. S.: An ectobiont-bearing foraminiferan,
473 Bolivina pacifica, that inhabits microxic pore waters: cell-biological and paleoceanographic
474 insights, Environmental Microbiology, 12, 2107-2119, 10.1111/j.1462-2920.2009.02073.x,
475 2010.

476 Carrier, V., Svenning, M. M., Gründger, F., Niemann, H., Dessandier, P.-A., Panieri, G., and
477 Kalenitchenko, D.: The Impact of Methane on Microbial Communities at Marine Arctic Gas
478 Hydrate Bearing Sediment, Frontiers in Microbiology, 11, 10.3389/fmicb.2020.01932, 2020.

479 Cedhagen, T.: Retention of chloroplasts and bathymetric distribution in the sublittoral
480 foraminiferan Nonionellina labradorica, Ophelia, 33, 17-30,
481 <https://doi.org/10.1080/00785326.1991.10429739>, 1991.

482 Charrieau, L. M., Ljung, K., Schenk, F., Daewel, U., Kritzberg, E., and Filipsson, H. L.: Rapid
483 environmental responses to climate-induced hydrographic changes in the Baltic Sea entrance,
484 Biogeosciences, 16, 3835-3852, 10.5194/bg-16-3835-2019, 2019.

485 Choquel, C., Geslin, E., Metzger, E., Filipsson, H. L., Risgaard-Petersen, N., Launeau, P.,
486 Giraud, M., Jauffrais, T., Jesus, B., and Mouret, A.: Denitrification by benthic foraminifera and
487 their contribution to N-loss from a fjord environment, Biogeosciences, 18, 327-341, 10.5194/bg-
488 18-327-2021, 2021.

489 Chronopoulou, P.-M., Salonen, I., Bird, C., Reichart, G.-J., and Koho, K. A.: Metabarcoding
490 insights into the trophic behavior and identity of intertidal benthic foraminifera, *Frontiers in*
491 *microbiology*, 10, 1169, <https://doi.org/10.3389/fmicb.2019.01169>, 2019.

492 Consolaro, C., Rasmussen, T., Panieri, G., Mienert, J., Bünz, S., and Szytybor, K.: Carbon isotope
493 ($\delta^{13}\text{C}$) excursions suggest times of major methane release during the last 14 kyr in Fram Strait,
494 the deep-water gateway to the Arctic, *Clim. Past*, 11, 669-685, [https://doi.org/10.5194/cp-11-](https://doi.org/10.5194/cp-11-669-2015)
495 [669-2015](https://doi.org/10.5194/cp-11-669-2015), 2015.

496 Darling, K. F., Schweizer, M., Knudsen, K. L., Evans, K. M., Bird, C., Roberts, A., Filipsson, H.
497 L., Kim, J.-H., Gudmundsson, G., Wade, C. M., Sayer, M. D. J., and Austin, W. E. N.: The
498 genetic diversity, phylogeography and morphology of Elphidiidae (Foraminifera) in the
499 Northeast Atlantic, *Mar. Micropaleontol.*, 129, 1-23,
500 <https://doi.org/10.1016/j.marmicro.2016.09.001>, 2016.

501 Dessandier, P.-A., Borrelli, C., Kalenitchenko, D., and Panieri, G.: Benthic Foraminifera in
502 Arctic Methane Hydrate Bearing Sediments, *Frontiers in Marine Science*, 6,
503 <https://doi.org/10.3389/fmars.2019.00765>, 2019.

504 Egger, M., Riedinger, N., Mogollón, J. M., and Jørgensen, B. B.: Global diffusive fluxes of
505 methane in marine sediments, *Nature Geoscience*, 11, 421-425, 10.1038/s41561-018-0122-8,
506 2018.

507 Fossile, E., Nardelli, M. P., Jouini, A., Lansard, B., Pusceddu, A., Moccia, D., Michel, E., Péron,
508 O., Howa, H., and Mojtahid, M.: Benthic foraminifera as tracers of brine production in
509 Storfjorden “sea ice factory”, *Biogeosciences*, 17, <https://doi.org/10.5194/bg-17-1933-2020>,
510 2020.

511 Frail-Gauthier, J. L., Mudie, P. J., Simpson, A. G. B., and Scott, D. B.: Mesocosm and
512 Microcosm Experiments On the Feeding of Temperate Salt Marsh Foraminifera, *J. Foraminifer.*
513 *Res.*, 49, 259-274, <https://doi.org/10.2113/gsjfr.49.3.259>, 2019.

514 Goldstein, S. T. and Corliss, B. H.: Deposit feeding in selected deep-sea and shallow-water
515 benthic foraminifera, *Deep Sea Research Part I: Oceanographic Research Papers*, 41, 229-241,
516 [https://doi.org/10.1016/0967-0637\(94\)90001-9](https://doi.org/10.1016/0967-0637(94)90001-9), 1994.

517 Gouy, M., Guindon, S., and Gascuel, O.: SeaView version 4: a multiplatform graphical user
518 interface for sequence alignment and phylogenetic tree building, *Mol. Biol. Evol.*, 27, 221-224,
519 <https://doi.org/10.1093/molbev/msp259>, 2010.

520 Hald, M. and Korsun, S.: Distribution of modern benthic foraminifera from fjords of Svalbard,
521 European Arctic, *The Journal of Foraminiferal Research*, 27, 101-122,
522 <https://doi.org/10.2113/gsjfr.27.2.101>, 1997.

- 523 Heinz, P., Geslin, E., and Hemleben, C.: Laboratory observations of benthic foraminiferal cysts,
524 Mar. Biol. Res., 1, 149-159, 2005.
- 525 Hemleben, C., Spindler, M., and Anderson, O. R.: Modern planktonic foraminifera, Springer
526 Science & Business Media 2012.
- 527 Herguera, J. C., Paull, C. K., Perez, E., Ussler III, W., and Peltzer, E.: Limits to the sensitivity of
528 living benthic foraminifera to pore water carbon isotope anomalies in methane vent
529 environments, *Paleoceanography*, 29, 273-289, <https://doi.org/10.1002/2013PA002457>, 2014.
- 530 Hill, R., Schreiber, U., Gademann, R., Larkum, A. W. D., Kuhl, M., and Ralph, P. J.: Spatial
531 heterogeneity of photosynthesis and the effect of temperature-induced bleaching conditions in
532 three species of corals, *Marine Biology*, 144, 633-640, [https://doi.org/10.1007/s00227-003-1226-](https://doi.org/10.1007/s00227-003-1226-1)
533 [1](https://doi.org/10.1007/s00227-003-1226-1), 2004a.
- 534 Hill, T. M., Kennett, J. P., and Valentine, D. L.: Isotopic evidence for the incorporation of
535 methane-derived carbon into foraminifera from modern methane seeps, Hydrate Ridge,
536 Northeast Pacific, *Geochimica et Cosmochimica Acta*, 68, 4619-4627,
537 <https://doi.org/10.1016/j.gca.2004.07.012>, 2004b.
- 538 Hinrichs, K.-U., Hmelo, L. R., and Sylva, S. P.: Molecular fossil record of elevated methane
539 levels in late Pleistocene coastal waters, *Science*, 299, 1214-1217,
540 <https://doi.org/10.1126/science.1079601>, 2003.
- 541 Holzmann, M. and Pawlowski, J.: An updated classification of rotaliid foraminifera based on
542 ribosomal DNA phylogeny, *Mar. Micropaleontol.*, 132, 18-34,
543 <https://doi.org/10.1016/j.marmicro.2017.04.002>, 2017.
- 544 Hong, W.-L., Torres, M. E., Carroll, J., Crémière, A., Panieri, G., Yao, H., and Serov, P.:
545 Seepage from an arctic shallow marine gas hydrate reservoir is insensitive to momentary ocean
546 warming, *Nat. Commun.*, 8, 15745, <https://doi.org/10.1038/ncomms15745>, 2017.
- 547 Hong, W. L., Torres, M. E., Portnov, A., Waage, M., Haley, B., and Lepland, A.: Variations in
548 gas and water pulses at an Arctic seep: fluid sources and methane transport, *Geophys. Res. Lett.*,
549 45, 4153-4162, <https://doi.org/10.1029/2018GL077309>, 2018.
- 550 Iversen, N. and Jørgensen, B. B.: Diffusion coefficients of sulfate and methane in marine
551 sediments: Influence of porosity, *Geochimica et Cosmochimica Acta*, 57, 571-578,
552 [https://doi.org/10.1016/0016-7037\(93\)90368-7](https://doi.org/10.1016/0016-7037(93)90368-7), 1993.
- 553 Jauffrais, T., LeKieffre, C., Schweizer, M., Jesus, B., Metzger, E., and Geslin, E.: Response of a
554 kleptoplastidic foraminifer to heterotrophic starvation: photosynthesis and lipid droplet
555 biogenesis, *FEMS Microbiol. Ecol.*, 95, 10.1093/femsec/fiz046, 2019a.

- 556 Jauffrais, T., LeKieffre, C., Schweizer, M., Geslin, E., Metzger, E., Bernhard, J. M., Jesus, B.,
557 Filipsson, H. L., Maire, O., and Meibom, A.: Kleptoplastic benthic foraminifera from aphotic
558 habitats: insights into assimilation of inorganic C, N and S studied with sub-cellular resolution,
559 *Environmental microbiology*, 21, 125-141, <https://doi.org/10.1111/1462-2920.14433>, 2019b.
- 560 Lee, J. J. and Muller, W. A.: Trophic dynamics and niches of salt marsh foraminifera, *Am. Zool.*,
561 13, 215-223, 1973.
- 562 Lee, J. J., McEnery, M., Pierce, S., Freudenthal, H., and Muller, W.: Tracer experiments in
563 feeding littoral foraminifera, *The Journal of Protozoology*, 13, 659-670, 1966.
- 564 LeKieffre, C., Bernhard, J. M., Mabilieu, G., Filipsson, H. L., Meibom, A., and Geslin, E.: An
565 overview of cellular ultrastructure in benthic foraminifera: New observations of rotalid species in
566 the context of existing literature, *Mar. Micropaleontol.*, 138, 12-32,
567 <https://doi.org/10.1016/j.marmicro.2017.10.005>, 2018.
- 568 Leutenegger, S. and Hansen, H. J.: Ultrastructural and radiotracer studies of pore function in
569 foraminifera, *Marine Biology*, 54, 11-16, 10.1007/BF00387046, 1979.
- 570 Lipps, J. H.: Biotic Interactions in Benthic Foraminifera, in: *Biotic Interactions in Recent and*
571 *Fossil Benthic Communities*, edited by: Tevesz, M. J. S., and McCall, P. L., Springer US,
572 Boston, MA, 331-376, 10.1007/978-1-4757-0740-3_8, 1983.
- 573 Mackensen, A.: On the use of benthic foraminiferal $\delta^{13}\text{C}$ in palaeoceanography: constraints
574 from primary proxy relationships, *Geological Society, London, Special Publications*, 303, 121-
575 133, <https://doi.org/10.1144/SP303.9>, 2008.
- 576 Mojtahid, M., Zubkov, M. V., Hartmann, M., and Gooday, A. J.: Grazing of intertidal benthic
577 foraminifera on bacteria: Assessment using pulse-chase radiotracing, *J. Exp. Mar. Biol. Ecol.*,
578 399, 25-34, <https://doi.org/10.1016/j.jembe.2011.01.011>, 2011.
- 579 Muller, W. A. and Lee, J. J.: Apparent Indispensability of Bacteria in Foraminiferan Nutrition,
580 *The Journal of Protozoology*, 16, 471-478, <https://doi.org/10.1111/j.1550-7408.1969.tb02303.x>,
581 1969.
- 582 Nomaki, H., Heinz, P., Nakatsuka, T., Shimanaga, M., and Kitazato, H.: Species-specific
583 ingestion of organic carbon by deep-sea benthic foraminifera and meiobenthos: In situ tracer
584 experiments, *Limnol. Oceanogr.*, 50, 134-146, <https://doi.org/10.4319/lo.2005.50.1.0134>, 2005.
- 585 Nomaki, H., Heinz, P., Nakatsuka, T., Shimanaga, M., Ohkouchi, N., Ogawa, N. O., Kogure, K.,
586 Ikemoto, E., and Kitazato, H.: Different ingestion patterns of C-13-labeled bacteria and algae by
587 deep-sea benthic foraminifera, *Marine Ecology-Progress Series*, 310, 95-108,
588 <https://doi.org/10.3354/meps310095>, 2006.

589 Nomaki, H., Bernhard, J. M., Ishida, A., Tsuchiya, M., Uematsu, K., Tame, A., Kitahashi, T.,
590 Takahata, N., Sano, Y., and Toyofuku, T.: Intracellular Isotope Localization in *Ammonia* sp.
591 (Foraminifera) of Oxygen-Depleted Environments: Results of Nitrate and Sulfate Labeling
592 Experiments, *Frontiers in Microbiology*, 7, <https://doi.org/10.3389/fmicb.2016.00163>, 2016.

593 Panieri, G.: Foraminiferal response to an active methane seep environment: A case study from
594 the Adriatic Sea, *Mar. Micropaleontol.*, 61, 116-130,
595 <https://doi.org/10.1016/j.marmicro.2006.05.008>, 2006.

596 Panieri, G., James, R. H., Camerlenghi, A., Westbrook, G. K., Consolaro, C., Cacho, I., Cesari,
597 V., and Cervera, C. S.: Record of methane emissions from the West Svalbard continental margin
598 during the last 23.500yrs revealed by $\delta^{13}\text{C}$ of benthic foraminifera, *Global and Planetary*
599 *Change*, 122, 151-160, <https://doi.org/10.1016/j.gloplacha.2014.08.014>, 2014.

600 Panieri, G., Lepland, A., Whitehouse, M. J., Wirth, R., Raanes, M. P., James, R. H., Graves, C.
601 A., Crémière, A., and Schneider, A.: Diagenetic Mg-calcite overgrowths on foraminiferal tests in
602 the vicinity of methane seeps, *Earth and Planetary Science Letters*, 458, 203-212,
603 <https://doi.org/10.1016/j.epsl.2016.10.024>, 2017.

604 Pascal, P.-Y., Dupuy, C., Richard, P., and Niquil, N.: Bacterivory in the common foraminifer
605 *Ammonia tepida*: Isotope tracer experiment and the controlling factors, *J. Exp. Mar. Biol. Ecol.*,
606 359, 55-61, <https://doi.org/10.1016/j.jembe.2008.02.018>, 2008.

607 Pawlowski, J.: Introduction to the molecular systematics of foraminifera, *Micropaleontology*, 46,
608 1-12, 2000.

609 Rathburn, A. E., Pérez, M. E., Martin, J. B., Day, S. A., Mahn, C., Gieskes, J., Ziebis, W.,
610 Williams, D., and Bahls, A.: Relationships between the distribution and stable isotopic
611 composition of living benthic foraminifera and cold methane seep biogeochemistry in Monterey
612 Bay, California, *Geochemistry, Geophysics, Geosystems*, 4, 2003.

613 Risgaard-Petersen, N., Langezaal, A. M., Ingvardsen, S., Schmid, M. C., Jetten, M. S. M., Op
614 den Camp, H. J. M., Derksen, J. W. M., Piña-Ochoa, E., Eriksson, S. P., Peter Nielsen, L., Peter
615 Revsbech, N., Cedhagen, T., and van der Zwaan, G. J.: Evidence for complete denitrification in a
616 benthic foraminifer, *Nature*, 443, 93, <https://doi.org/10.1038/nature05070>, 2006.

617 Salonen, I. S., Chronopoulou, P.-M., Bird, C., Reichart, G.-J., and Koho, K. A.: Enrichment of
618 intracellular sulphur cycle-associated bacteria in intertidal benthic foraminifera revealed by 16S
619 and aprA gene analysis, *Sci Rep-Uk*, 9, 1-12, <https://doi.org/10.1038/s41598-019-48166-5>, 2019.

620 Schneider, A., Crémière, A., Panieri, G., Lepland, A., and Knies, J.: Diagenetic alteration of
621 benthic foraminifera from a methane seep site on Vestnesa Ridge (NW Svalbard), *Deep Sea*
622 *Research Part I: Oceanographic Research Papers*, 123, 22-34,
623 <https://doi.org/10.1016/j.dsr.2017.03.001>, 2017.

- 624 Serov, P., Vadakkepuliambatta, S., Mienert, J., Patton, H., Portnov, A., Silyakova, A., Panieri,
625 G., Carroll, M. L., Carroll, J., Andreassen, K., and Hubbard, A.: Postglacial response of Arctic
626 Ocean gas hydrates to climatic amelioration, *Proceedings of the National Academy of Sciences*,
627 114, 6215-6220, 10.1073/pnas.1619288114, 2017.
- 628 Shetye, S., Mohan, R., Shukla, S. K., Maruthadu, S., and Ravindra, R.: Variability of
629 *Nonionellina labradorica* Dawson in Surface Sediments from Kongsfjorden, West Spitsbergen,
630 *Acta Geologica Sinica - English Edition*, 85, 549-558, [https://doi.org/10.1111/j.1755-
631 6724.2011.00450.x](https://doi.org/10.1111/j.1755-6724.2011.00450.x), 2011.
- 632 Tavormina, P. L., Hatzepichler, R., McGlynn, S., Chadwick, G., Dawson, K. S., Connon, S. A.,
633 and Orphan, V. J.: *Methyloprofundus sedimenti* gen. nov., sp. nov., an obligate methanotroph
634 from ocean sediment belonging to the 'deep sea-1' clade of marine methanotrophs, *Int. J. Syst.*
635 *Evol. Microbiol.*, 65, 251-259, <https://doi.org/10.1099/ijs.0.062927-0>, 2015.
- 636 Torres, M. E., Martin, R. A., Klinkhammer, G. P., and Nesbitt, E. A.: Post depositional alteration
637 of foraminiferal shells in cold seep settings: New insights from flow-through time-resolved
638 analyses of biogenic and inorganic seep carbonates, *Earth and Planetary Science Letters*, 299,
639 10-22, <https://doi.org/10.1016/j.epsl.2010.07.048>, 2010.
- 640 Wefer, G., Heinze, P. M., and Berger, W. H.: Clues to ancient methane release, *Nature*, 369, 282,
641 <https://doi.org/10.1038/369282a0>, 1994.
- 642 Wollenburg, J. E., Raitzsch, M., and Tiedemann, R.: Novel high-pressure culture experiments on
643 deep-sea benthic foraminifera—Evidence for methane seepage-related $\delta^{13}\text{C}$ of *Cibicides*
644 *wuellerstorfi*, *Mar. Micropaleontol.*, 117, 47-64, 2015.
645